EVALUATION OF CLOSED CUBIC FAILURE CRITERION FOR GRAPHITE/EPOXY LAMINATES

R. C. Tennyson and Zhiqing Jiang

Final Report Submitted to

NASA Langley Research Center

Under Grant No. NAGW-752

APRIL 1987

ACKNOWLEDGEMENTS

The authors would like to acknowledge the financial aid of the Natural Sciences and Engineering Research Council of Canada (Grant No. A-2783) who have provided a valuable supplement to the support received from the U.S. National Aeronautics and Space Administration (under Grant No. NAGW-752) for the development of the static strength model. We are also very appreciative to Mr. Don Baker for his continued interest in our work. Finally, we would like to express our appreciation to the Shijiazhuang Railway Institute of China for permitting Mr. Zhiqing Jiang to work at UTIAS.

Abstract

An analytical method has been developed to ensure closure of the cubic form of the tensor polynomial strength criterion. The intrinsic complexity of the cubic function is such that special conditions must be met to close the failure surface in three-dimensional stress space. These requirements are derived in terms of non-intersecting conditions for asymptotes and an asymptotic plane. To demonstrate the validity of this approach, closed failure surfaces were derived for two graphite/epoxy material systems (3M SP288-T300 and IM7 8551-7). The agreement of test data with this model clearly shows that it is possible to use a higher order cubic failure theory with confidence.

Table of Contents

Nomenclature

F_i, F_{ij}, F_{ijk}	Strength tensors
F_{12}	Quadratic interaction strength parameter
F_{112}, F_{122}, F_{166}, F_{266}	Cubic interaction strength parameters
S, S'	Positive and negative shear strengths measured in the 1-2 plane
X, X'	Tensile and compressive strengths measured along the fiber (1) axis, respectively
Y, Y'	Tensile and compressive strengths measured in the direction orthogonal to fibers (2)
σ_1, σ_2	Normal plane stresses along the 1 and 2 axes, respectively
σ_6	Shear stress measured in the 1-2 plane

1. INTRODUCTION

With the advent of composite material primary structural components in advanced high performance aircraft and helicopters, the need for proven predictive formulations to quantify the strength of laminates is of paramount concern. In aerospace construction, one usually encounters relatively thin-walled structures and thus, to a first approximation, a plane stress state can be assumed to exist for preliminary design purposes. However, it is becoming increasingly evident that in many instances, three-dimensional stress effects must be considered, particularly in the vicinity of free edges (associated with joints, cutouts, fasteners, etc.). Indeed, such effects can lead to delamination and/or crack initiation which are of major interest to the analyst. Regardless of the stress state, the requirements for lamina and overall structural failure criteria still persist. The most desirable failure model is one which can provide conservative maximum load estimates of reliable accuracy. However, the model must not be so conservative that it jeopardizes the design itself in terms of increasing the weight needlessly. On the other hand, it should be relatively operationally easy to employ, and not be dependent on the development of such an extensive data base using complex and expensive test procedures that the user shuns its application. One might comment that the presence of local stress concentrations (due to cracks, free edges, holes, etc.) does not influence the form of a lamina strength criterion. Rather, such considerations can be taken into account in the formulation of the stress analysis and the failure criterion one adopts for the whole laminate. For example, if one is performing a finite element analysis, including three-dimensional stress terms, failure is determined not only by the lamina failure model, but equally as important, by the laminate failure model one assumes.

Lamina failure models can essentially be grouped into three categories of increasing operational complexity. The simplest approach is to design to maximum stress or strain (which are not equivalent criteria). Unfortunately, these models lead to substantial "over-estimates" of strength in the "corner" regions of the failure surface envelope. The next class of models are those which approximate the failure surface by quadratic polynomials of different forms. Many variations of quadratic models can be found in the literature, including ones which define the surface using different functions for each quadrant. Again, it has been demonstrated that, for certain load cases, quadratic formulations can overestimate strength as well (Ref. 1). In some instances, such as biaxial loading, the quadratic criterion can under-predict strength by as much as 30%-40% (Ref. 2). The third category of failure criteria is termed "higher order models", the most common one of which is the "cubic" polynomial (Refs. 1, 2, 3). It should be noted that all of the above mentioned formulations represent approximations encompassed by the general "tensor polynomial" criterion advocated in Ref. 3. The one feature that is common to all of these lamina failure models is that they represent a phenomenological, macro-mechanics approach to predicting lamina failure. They all attempt to describe the real failure surface in stress (or strain) space. Table 1 presents a summary of the test data and interaction strength parameters that one would require for each classification of failure model. It becomes quite apparent that the higher order cubic model demands more baseline strength data. This of course raises the question as to whether or not the additional complexity (and cost) is warranted. As noted earlier, there do exist regions of the failure surface (for a plane stress state) where indeed such a criterion is required. However, it should also be noted that recent work has shown that for laminates fabricated from orthogonal woven fabric

prepreg materials, a quadratic model provides quite accurate strength predictions even under biaxial stress states (Refs. 4, 5). One of the main difficulties encountered when attempting to 'model' the failure surface with a single cubic polynomial representation is due to the mathematical nature of the cubic equation. It has been found in previous work that the failure surface in stress space (σ_1, σ_2, σ_6) is not necessarily closed and hence situations can occur where 'infinite' strengths are predicted. For example, this was observed in earlier work (Refs. 6, 7) in the compression-compression quadrant where experimental data were not available to assist in the evaluation of the strength coefficients.

To overcome this problem of 'openness' of the failure surface, a new approach was taken with a view to establishing the necessary criteria to ensure 'local' closure of the cubic polynomial. It is well known that some cubic curves, such as the 'Folium of Descartes' (i.e., $x^3 + y^3 - 3axy = 0$), possess a locally closed region. It is shown in the following report that indeed the cubic form of the tensor polynomial failure surface can be closed providing one satisfies certain criteria associated with asymptotes of the image of this function. Such closure conditions are presented and the model is successfully applied to two different composite material systems.

2. ANALYTICAL MODEL

The most general failure criterion available for unflawed composite materials is the tensor polynomial which was advocated as early as 1966 by Malmeister (Ref. 8) and developed extensively by Tsai and Wu (Ref. 3) in quadratic and higher order forms. The failure surface in stress space can be described by the equation,

$$F_i\sigma_i + F_{ij}\sigma_i\sigma_j + F_{ijk}\sigma_i\sigma_j\sigma_k + \ldots = f(\sigma) \begin{cases} < 1 \text{ no failure} \\ = 1 \text{ failure} \\ > 1 \text{ exceeded failure} \end{cases} \quad (1)$$

for i, j, k = 1...6. F_i, F_{ij} and F_{ijk} are strength tensors of the 2nd, 4th and 6th rank, respectively.

Plane Stress State

If one restricts the analysis to a plane stress state and considers only a cubic formulation as being a reasonable representation of the failure surface, then Eq. (1) can be reduced to

$$F_1\sigma_1 + F_2\sigma_2 + F_{11}\sigma_1^2 + F_{22}\sigma_2^2 + F_{66}\sigma_6^2 + 2F_{12}\sigma_1\sigma_2 + 3F_{112}\sigma_1^2\sigma_2 + 3F_{122}\sigma_2^2\sigma_1 + 3F_{166}\sigma_1\sigma_6^2 + 3F_{266}\sigma_2\sigma_6^2 = 1 \quad (2)$$

From the analysis by Wu (Ref. 9), it was shown that the principal strength tensor components (F_i and F_{ii}) can be readily calculated from the experimentally determined values of the uniaxial tensile and compressive failure stresses in the fiber direction (X and X'), perpendicular to the fibers (Y and Y') and from positive and negative pure shear failure stresses (S and S', respectively). The appropriate relations are given by:

$$F_1 = \frac{1}{X} - \frac{1}{X'} \qquad F_2 = \frac{1}{Y} - \frac{1}{Y'} \qquad F_6 = 0$$

$$F_{11} = \frac{1}{XX'} \qquad F_{22} = \frac{1}{YY'} \qquad F_{66} = \frac{1}{S^2} \quad (3)$$

where for the materials considered, S = S'.

The problem that one is confronted with is the evaluation of the remaining interaction strength parameters such that Eq. (2) yields a

'locally closed' failure surface. This can be accomplished in two stages. First, let us re-write Eq. (2) in the form,

$$\sigma_6^2 = \frac{-(F_1\sigma_1 + F_2\sigma_2 + F_{11}\sigma_1^2 + F_{22}\sigma_2^2 + 2F_{12}\sigma_1\sigma_2 + 3F_{112}\sigma_1^2\sigma_2 + 3F_{122}\sigma_1\sigma_2^2 - 1)}{F_{66} + 3F_{166}\sigma_1 + 3F_{266}\sigma_2} \quad (4)$$

It is now possible to formulate the conditions for closure:

(a) ensure that the cubic curve describing the intersecting σ_1-σ_2 plane is closed.

(b) for given values of σ_1, σ_2, real values for σ_6 must exist; thus the asymptotic plane defined by

$$F_{66} + 3F_{166}\sigma_1 + 3F_{266}\sigma_2 = 0$$

cannot intersect the cubic curve in (a).

Condition (a)

To satisfy condition (a), one must examine the crossing of the failure surface on the σ_1-σ_2 plane, which occurs when $\sigma_6 = 0$. This yields the cubic equation

$$F_1\sigma_1 + F_2\sigma_2 + F_{11}\sigma_1^2 + F_{22}\sigma_2^2 + 2F_{12}\sigma_1\sigma_2 + 3F_{112}\sigma_1^2\sigma_2 + 3F_{122}\sigma_1\sigma_2^2 - 1 = 0 \quad (5)$$

Noting that the principal strength parameters are given by Eq. (3), it is necessary at this point to set up criteria that must be satisfied by the interaction terms F_{12}, F_{112} and F_{122}. These can be constructed by examining the asymptotes of Eq. (5), which can readily be obtained if one re-writes

the equation as a quadratic in either σ_1 or σ_2. The corresponding asymptotes are given by,

$$3F_{122}\sigma_1 + F_{22} = 0 \tag{6a}$$

$$3F_{112}\sigma_2 + F_{11} = 0 \tag{6b}$$

$$3F_{112}^2 F_{122}\sigma_1 + 3F_{112}F_{122}^2\sigma_2 = F_{11}F_{122}^2 + F_{22}F_{112}^2 - 2F_{12}F_{112}F_{122} \tag{6c}$$

Closure of the curve (5) results if none of the asymptotes (Eq. (6)) passes through the defined region. Hence the following conditions (derived from Eq. (5)) are necessary to ensure closure:

$$\begin{aligned}
&-\frac{F_{22}}{3F_{122}} < -X' \quad (\text{if } F_{122} > 0) \quad \text{or} \quad -\frac{F_{22}}{3F_{122}} > X \quad (\text{if } F_{122} < 0) \\
&-\frac{F_{11}}{3F_{112}} < -Y' \quad (\text{if } F_{112} > 0) \quad \text{or} \quad -\frac{F_{11}}{3F_{112}} > Y \quad (\text{if } F_{112} < 0) \\
&\frac{T}{F_{112}} < -X' \quad \left(\text{if } \frac{T}{F_{112}} < 0\right) \quad \text{or} \quad \frac{T}{F_{112}} > X \quad \left(\text{if } \frac{T}{F_{112}} > 0\right) \\
&\frac{T}{F_{122}} < -Y' \quad \left(\text{if } \frac{T}{F_{122}} < 0\right) \quad \text{or} \quad \frac{T}{F_{122}} > Y \quad \left(\text{if } \frac{T}{F_{122}} > 0\right)
\end{aligned} \tag{7}$$

where

$$T = \frac{F_{11}F_{122}^2 + F_{22}F_{112}^2 - 2F_{12}F_{112}F_{122}}{3F_{112}F_{122}}$$

Evaluation of F_{12}, F_{112}, F_{122}

Suppose one performs a set of 'n' biaxial load tests (i.e., with $\sigma_6 = 0$) to generate 'n' data sets $(\sigma_{1i}, \sigma_{2i})$ $(i = 1, 2, \ldots n)$. Note that

the uniaxial tests required to evaluate the principal strength parameters in Eq. (3) are excluded. Using these data it is possible to evaluate F_{12}, F_{112} and F_{122} by a least-squares fit of the cubic Eq. (5). This simple approach is often sufficient to produce a closed curve in σ_1-σ_2 space (thus satisfying the criteria of Eq. (7)), as will be demonstrated later.

If closure does not occur, then removal of one or more of the asymptotes from intersecting the failure plane is required. To demonstrate how this can be done, let us consider the following example. Suppose the following asymptote

$$3F_{122}\sigma_1 + F_{22} = 0$$

penetrates the cubic curve (Eq. (5)) between (-X', 0, 0) and the origin. Clearly, by shifting it to the left of the line $\sigma_1 + X' = 0$ will lead to closure. In the limiting case when the asymptote is allowed to pass through (-X', 0, 0), it then becomes a part of the failure curve. The cubic curve thus degenerates into a quadratic curve and a straight line.

Substituting $\sigma_1 = -X'$ into Eq. (5) gives

$$(-3F_{122}X' + F_{22})\sigma_2^2 + (3F_{112}X'^2 - 2F_{12}X' + F_2)\sigma_2 + (F_{11}X'^2 - F_1X' - 1) = 0 \qquad (8)$$

As there must exist an infinity of roots, σ_2, then the following conditions hold:

$$-3F_{122}X' + F_{22} = 0 \qquad (9)$$

$$3F_{112}X'^2 - 2F_{12}X' + F_2 = 0 \qquad (10)$$

$$F_{11}X'^2 - F_1X' - 1 = 0 \tag{11}$$

Equation (11) is the solution one obtains by setting $\sigma_2 = \sigma_6 = 0$ and $\sigma_1 = -X'$ in Eq. (2). This leads to the results shown in Eq. (3) for F_1 and F_{11} as derived in Ref. 9. Equations (9) and (10) define constraint conditions that must now be met by F_{12}, F_{112} and F_{122}. One may now proceed to use the method of Lagrange multipliers to incorporate these 'side conditions' in evaluating the least-squares best fit curve to the available test data. This is accomplished by formulating the following functional:

$$F = \sum_{i=1}^{n} (F_1\sigma_{1i} + F_2\sigma_{2i} + F_{11}\sigma_{1i}^2 + F_{22}\sigma_{2i}^2 + 2F_{12}\sigma_{1i}\sigma_{2i}$$

$$+ 3F_{112}\sigma_{1i}^2\sigma_{2i} + 3F_{122}\sigma_{1i}\sigma_{2i}^2 - 1)^2$$

$$+ \lambda_1(-3F_{122}X' + F_{22}) + \lambda_2(3F_{112}X'^2 - 2F_{12}X' + F_2) \tag{12}$$

where λ_1, λ_2 are Lagrangian multipliers,

F_1, F_2, F_{11}, F_{22} are determined by experiment (see Eq. (3)). The minimum value of 'F' yielding a "best" least squares fit is obtained from

$$\frac{\partial F}{\partial F_{12}} = 4 \sum_{i=1}^{n} \sigma_{1i}\sigma_{2i}(F_1\sigma_{1i} + F_2\sigma_{2i} + F_{11}\sigma_{1i}^2 + F_{22}\sigma_{2i}^2 + 2F_{12}\sigma_{1i}\sigma_{2i}$$

$$+ 3F_{112}\sigma_{1i}^2\sigma_{2i} + 3F_{122}\sigma_{1i}\sigma_{2i}^2 - 1) - 2X'\lambda_2 = 0 \tag{13}$$

$$\frac{\partial F}{\partial F_{112}} = 6 \sum_{i=1}^{n} \sigma_{1i}{}^2\sigma_{2i}(F_1\sigma_{1i} + F_2\sigma_{2i} + F_{11}\sigma_{1i}{}^2 + F_{22}\sigma_{2i}{}^2 + 2F_{12}\sigma_{1i}\sigma_{2i}$$

$$+ 3F_{112}\sigma_{1i}{}^2\sigma_{2i} + 3F_{122}\sigma_{1i}\sigma_{2i}{}^2 - 1) + 3X'^2\lambda_2 = 0 \qquad (14)$$

$$\frac{\partial F}{\partial F_{122}} = 6 \sum_{i=1}^{n} \sigma_{1i}\sigma_{2i}{}^2(F_1\sigma_{1i} + F_2\sigma_{2i} + F_{11}\sigma_{1i}{}^2 + F_{22}\sigma_{2i}{}^2 + 2F_{12}\sigma_{1i}\sigma_{2i}$$

$$+ 3F_{112}\sigma_{1i}{}^2\sigma_{2i} + 3F_{122}\sigma_{1i}\sigma_{2i}{}^2 - 1) - 3X'\lambda_1 = 0 \qquad (15)$$

$$\frac{\partial F}{\partial \lambda_1} = -3F_{122}X' + F_{22} = 0 \qquad (16)$$

$$\frac{\partial F}{\partial \lambda_2} = 3F_{112}X'^2 - 2F_{12}X' + F_2 = 0 \qquad (17)$$

Resolving the simultaneous equations (13)-(17), one can obtain F_{12}, F_{112} and F_{122}. Thus one can now construct a closed cubic curve (Eq. (5)) that represents a 'best fit' to test data.

Finally one should note that if 'openness' of the cubic curve (5) occurs in a different quadrant, then the same procedures can be applied by substituting different values for σ_1 or σ_2 into Eq. (5) to obtain the appropriate constraint equations.

Condition (b) - Evaluation of F_{166} and F_{266}

Closure of the cubic failure surface is dependent on the location of the plane defined by

$$F_{66} + 3F_{166}\sigma_1 + 3F_{266}\sigma_2 = 0 \qquad (18)$$

The image of Eq. (18) is a line on the σ_1-σ_2 plane as illustrated in Fig. 1, where the shaded areas shown represent the 'positive side' of the line (18), assuming $F_{66} > 0$, $F_{166} < 0$ and $F_{266} < 0$. In case (a) all points in the closed region are situated on the positive side and thus $\sigma_6^2 > 0$ (see Eq. (4)). Because $\sigma_6 = 0$ on the boundary of the closed region, and the function defined by Eq. (4) is continuous, one can conclude that the cubic failure surface is closed. Case (b) is opposite to (a) in that for every point (σ_1, σ_2) in the closed region, one cannot obtain a real value for σ_6. In this case, the failure surface is open above and below the closed region shown in the σ_1-σ_2 plane. This particular circumstance cannot actually occur because the points $(0, 0, \pm S)$ are located on the failure surface. Case (c) is more typical where a region of the failure surface (above the line) is open. As one approaches this line (Eq. (18)), $\sigma_6 \to \pm \infty$. Consequently, one can define the necessary condition for closure as:

the straight line (18) must not 'intersect' the closed cubic curve (5)

In general, one can derive the required constraint conditions for F_{166} and F_{266} by making the straight line (18) tangent to the cubic curve (5). The coordinates of the point of intersection can be calculated for these equations by first substituting for σ_2 (from Eq. (18)) into Eq. (5) to obtain

$$27(F_{122}F_{166}^2 - F_{112}F_{166}F_{266})\sigma_1^3 + 9(F_{11}F_{266}^2 + F_{22}F_{166}^2 - 2F_{12}F_{166}F_{266}$$

$$- F_{66}F_{112}F_{266} + 2F_{66}F_{122}F_{166})\sigma_1^2$$

$$+ 3(F_{66}^2F_{122} - 2F_{12}F_{66}F_{266} + 2F_{22}F_{66}F_{166} - 3F_2F_{166}F_{266} + 3F_1F_{266}^2)\sigma_1$$

$$+ (F_{22}F_{66}^2 - 3F_2F_{66}F_{266} - 9F_{266}^2) = 0 \qquad (19)$$

Because the tangent is a 'limit point' of the secant, then the σ_1-coordinate of the point of tangency will correspond to the repeat real roots of Eq. (19). Thus

$$\frac{1}{4}\left(\frac{2B^3 - 9ABC + 27A^2D}{27A^3}\right)^2 + \frac{1}{27}\left(\frac{3AC - B^2}{3A^2}\right)^3 = 0 \qquad (20)$$

where

$$A = 27(F_{122}F_{166}^2 - F_{112}F_{166}F_{266})$$

$$B = 9(F_{11}F_{266}^2 + F_{22}F_{166}^2 - 2F_{12}F_{166}F_{266} - F_{66}F_{112}F_{266} + 2F_{66}F_{122}F_{166})$$

$$C = 3(F_1F_{266}^2 - 3F_2F_{166}F_{266} + 2F_{22}F_{66}F_{166} - 2F_{12}F_{66}F_{266} + F_{66}^2F_{122})$$

$$D = F_{22}F_{66}^2 - 3F_2F_{66}F_{266} - 9F_{266}^2 \qquad (21)$$

Simplifying Eq. (20) yields the following constraint condition:

$$27A^2D^2 - 18ABCD + 4AC^3 - B^2C^2 + 4B^3D = 0 \qquad (22)$$

As in the previous analysis, one can use the Lagrange multiplier method and obtain the least squares 'best-fit' closed failure surface. Assuming one has 'n' data sets $(\sigma_{1i}, \sigma_{2i}, \sigma_{6i})$, $(i = 1, 2, \ldots n)$, the following functional can be formulated:

$$F = \sum_{i=1}^{n} (F_1\sigma_{1i} + F_2\sigma_{2i} + F_{11}\sigma_{1i}^2 + F_{22}\sigma_{2i}^2 + F_{66}\sigma_{6i}^2 + 2F_{12}\sigma_{1i}\sigma_{2i}$$

$$+ 3F_{112}\sigma_{1i}^2\sigma_{2i} + 3F_{122}\sigma_{1i}\sigma_{2i}^2 + 3F_{166}\sigma_{1i}\sigma_{6i}^2 + 3F_{266}\sigma_{2i}\sigma_{6i}^2 - 1)^2$$

$$+ \lambda(27A^2D^2 - 18ABCD + 4AC^3 - B^2C^2 + 4B^3D) \qquad (23)$$

where λ is a Lagrangian multiplier. 'F' can reach an extreme value only if

$$\frac{\partial F}{\partial F_{166}} = 0, \qquad \frac{\partial F}{\partial F_{266}} = 0, \qquad \frac{\partial F}{\partial \lambda} = 0 \qquad (24)$$

Thus one can obtain a set of nonlinear simultaneous equations that will yield a solution for F_{166} and F_{266}.

3. DERIVATION OF CLOSED FAILURE SURFACES

Graphite/Epoxy: 3M SP288 - T300

This material was first studied in Refs. 1, 10, 11 where it was found that the cubic failure surface was open in the compression-compression quadrant in the σ_1-σ_2 plane (see Fig. 2). The material properties used to derive this curve are contained in Tables 2-5. It should be noted that no biaxial test data were used, and as a result, two asymptotes (given by Eq. (6b), (6c)) were found to penetrate the failure curve, Eq. (5). Biaxial tests were then performed (see Table 6) and closure of the curve (Eq. (5)) was obtained, as is evident in Fig. 3. One can now see that all three asymptotes lie outside the failure plane. The corresponding modified coefficients F_{12}, F_{112} and F_{122} are given in Table 5. For comparison purposes, the 'original' and 'revised' failure curves are plotted in Fig. 4

together with the quadratic model which can be seen to significantly overestimate the failure stresses in the compression-compression quadrant. Thus it would appear that a minimum of three biaxial tests in the σ_1-σ_2 plane can be used to obtain a closed failure curve. However, subsequent analysis (Ref. 3) using these coefficients together with F_{166} and F_{266}, as determined in Refs. 1, 2, showed that the failure surface was 'open' in a limited region of σ_6 values (Fig. 5). It is interesting to note that Eq. (18) passes through the 'points of intersection' A and B (in Fig. 5). Thus, if one varies F_{166} and F_{266}, in the limiting case when A→B, Eq. (18) becomes the tangent plane and closure of the failure surface (Eq. (2)) occurs. Closure is only guaranteed if one imposes the constraint condition, Eq. (22). To demonstrate this, additional failure tests were conducted with σ_1-σ_6 and σ_2-σ_6 loading (see Table 6) and new estimates for F_{166} and F_{266} made. Using these revised coefficients (see Table 5) without imposing the constraint condition led to the results shown in Figs. 6 and 7 (i.e., an open failure surface). However, closure was obtained employing the same data and solving for F_{166} and F_{266} using Eqs. (23) and (24). The results of this analysis are presented in Figs. 8 and 9. Now one can see (Fig. 8) that Eq. (18) is indeed a tangent plane to the failure curve (Eq. (5)) and closure of the complete failure surface (Eq. (2)) was achieved (Fig. 9).

For comparison purposes, failure tests were undertaken using $(\pm\theta)_s$ laminated tubes subject to internal pressure loading. Figure 10 presents the test data (reported in Ref. 6) and the predicted strength curve using the coefficients of Table 5 for the 'closed' surface. The agreement is very good and for most cases, the model is somewhat conservative. Once again, however, it is clearly evident that the quadratic criterion is far too conservative, particularly in the 'optimal' fiber angle region.

Graphite/Epoxy: Hercules IM7/8551-7

A new graphite/epoxy material was investigated to determine its elastic and strength properties, the results of which are summarized in Tables 2 and 3, respectively. The corresponding principal strength parameters are given in Table 4. As in the previous case, a first estimate of the interaction strength coefficients was made based on the test data in Table 8. Least squares analysis was used but no constraint conditions were applied. The results of these calculations are presented in Table 5. It can be seen in Fig. 11 that the σ_1-σ_2 curve is closed (for $\sigma_6 = 0$) but that the straight line (18) does pass through the failure region. This of course leads to an open failure surface and indeed such is the case in Fig. 12 for a range of σ_6 loading.

However, if the constraint condition is imposed and F_{166}, F_{266} evaluated according to Eqs. (23) and (24), one does obtain a closed failure surface. This is first evident in Fig. 13 where the image of Eq. (18) is now a tangent to the σ_1-σ_2 curve. One can also see in Fig. 14 that the failure plane σ_2-σ_6 is closed. Finally, a series of failure planes shown in Fig. 15 clearly demonstrate that the whole failure surface is now closed. Note that in Figs. 13-15 some limited test results are included for comparison purposes, over and above the data employed to estimate the interaction strength parameters.

4. CONCLUSIONS

An analytical method has been presented utilizing constraint conditions that permits one to construct a closed cubic polynomial failure surface. The procedure is based on three stages of testing and analysis:

(1) Calculate the principal strength parameters (F_1, F_2, F_{11}, F_{22}, F_{66}) based on standard tension, compression and shear tests.

(2) Conduct biaxial load tests ($\sigma_6 = 0$) at a minimum of three different stress levels and evaluate the interaction parameters (F_{12}, F_{112}, F_{122}) in the cubic failure equation (5) in the σ_1-σ_2 plane using the method of least squares. If this failure curve is open, invoke closure conditions described in this report.

(3) Conduct combined loading tests involving shear stress preferably at two different stress levels and invoke the closure condition (Eq. (22)) to evaluate F_{166} and F_{266} using Eqs. (23), (24).

This report presents closed failure surfaces for two different graphite/epoxy materials using the methodology described. The analyst and designer now have available for the first time a closed form of the cubic polynomial failure criterion.

REFERENCES

1. Tennyson, R. C., Nanyaro, A. P., Wharram, G. E., "Application of the Cubic Polynomial Strength Criterion to the Failure Analysis of Composite Materials", J. Composite Materials Supplement, Vol. 14, 1980, pp. 28-41.

2. Tennyson, R. C., Elliott, W. G., "Failure Analysis of Composite Laminates Including Biaxial Compression", NASA CR 172192, Aug. 1983.

3. Tsai, S. W., Wu, E. M., "A General Theory of Strength for Anisotropic Materials", J. Composite Materials, Vol. 5, 1971.

4. Tennyson, R. C. and Wharram, G. E., "Development of Failure Criterion for Kevlar/Epoxy Fabric Laminates", NASA CR 172465, July 1984.

5. Tennyson, R. C. and Wharram, G. E., "Evaluation of Failure Criterion for Graphite/Epoxy Fabric Laminates", NASA CR 172547, Feb. 1985.

6. Tennyson, R. C., MacDonald, D., Nanyaro, A. P., "Evaluation of the Tensor Polynomial Failure Criterion for Composite Materials", J. Composite Materials, Vol. 12, 1978, pp. 63-75.

7. Nanyaro, A. P., "Evaluation of the Tensor Polynomial Failure Criterion for Composite Materials", M.A.Sc. Thesis, University of Toronto, 1978.

8. Malmeister, A. K., "Geometry of Theories of Strength", Mekhanika Polimerov, Vol. 2, No. 4, 1966.

9. Wu, E. M., "Optimal Experimental Measurements of Anisotropic Failure Tensors", J. Composite Materials, Vol. 6, 1972.

10. Tennyson, R. C., "Application of the Cubic Strength Criterion to the Failure Analysis of Composite Structures", NASA CR 165712, May 1981.

11. Tennyson, R. C., "Experimental Evaluation of the Tensor Polynomial Failure Criterion for Designing Composite Structures", NASA CR-155219, October 1977.

Table 1

Plane Stress Failure Model Test Requirements*

Failure Model	Test Requirements
Maximum Stress or Strain (1)	0° tension, compression 90° tension, compression 0° or 90° shear
Quadratic (2)	Same as (1) with option to evaluate interaction term F_{12} analytically (using "closure" condition) or with biaxial tension test
Cubic (3)	Minimum requirements: (a) 3 biaxial load tests $(\sigma_1-\sigma_2) \rightarrow F_{12}, F_{112}, F_{122}$ (b) Solve for F_{166} and F_{266} from constraint Eq. (22) and Eq. (2) based on 1 'shear' test using either $\sigma_1-\sigma_6$ or $\sigma_2-\sigma_6$ loading. Preferable: (a) + two 'shear' tests $(\sigma_1-\sigma_6)$ and $(\sigma_2-\sigma_6)$, and solving Eqs. (23), (24) for F_{166}, F_{266}

*These hold for an orthotropic material, such as unidirectional prepreg or woven (orthotropic) fabric. In the latter case 0° and 90° refer to warp and fill directions, respectively.

Table 2

Graphite/Epoxy Material Properties

Material	E_{11} GPa	E_{22} GPa	G_{12} GPa	ν_{12}
3M SP288-T300	141.35	9.65	4.10	0.260
Hercules IM7/8551-7	162.03	8.34	2.07	0.339

Table 3

Summary of Average Failure Strengths for Graphite/Epoxy Materials

Material	No. Tests	X MPa	X' MPa	Y MPa	Y' MPa	S=S' MPa
3M SP288 -T300	8	1279.92 ± 7%				
	4		876.25 ± 10%			
	5			51.82 ± 3%		
	4				233.07 ± 6%	
	6					95.88 ± 9%
Hercules IM7/8551-7	5	2417.39 ± 2%				
	5		1034.94 ± 6%			
	4			73.09 ± 1%		
	4				175.82 ± 4%	
	4					183.41 ± 10%

Note: % variation shown denotes maximum in number of samples tested.

Table 4

Summary of Principal Strength Parameters

Material	F_1 $(MPa)^{-1}$	F_{11} $(MPa)^{-2}$	F_2 $(MPa)^{-1}$	F_{22} $(MPa)^{-2}$	F_6 $(MPa)^{-1}$	F_{66} $(MPa)^{-2}$
3M SP288 -T300	-3.600×10^{-4}	8.917×10^{-7}	1.501×10^{-2}	8.279×10^{-5}	0	1.088×10^{-4}
Hercules IM7/8551-7	-5.526×10^{-4}	3.997×10^{-7}	7.994×10^{-3}	7.783×10^{-5}	0	2.972×10^{-5}

Table 5

Summary of Interaction Strength Parameters

Material	F_{12} $(MPa)^{-2}$	F_{112} $(MPa)^{-3}$	F_{122} $(MPa)^{-3}$	F_{166} $(MPa)^{-3}$	F_{266} $(MPa)^{-3}$
3M SP288-T300					
Original Est. (Refs. 1,10,11)	-9.306×10^{-6}	1.577×10^{-9}	-1.826×10^{-8}	-1.237×10^{-8}	-6.919×10^{-7}
Revised (Ref. 2)	-4.697×10^{-6}	-8.841×10^{-10}	-1.549×10^{-8}	-1.272×10^{-8}	-3.130×10^{-7}
Revised*	-4.697×10^{-6}	-8.841×10^{-10}	-1.549×10^{-8}	-7.090×10^{-9}	-7.032×10^{-7}
Closed Eqs. (23,24)	-4.697×10^{-6}	-8.841×10^{-10}	-1.549×10^{-8}	6.147×10^{-8}	-5.415×10^{-7}
Hercules IM7/8551-7					
First Est.**	8.412×10^{-7}	-1.243×10^{-9}	1.627×10^{-8}	4.939×10^{-8}	4.482×10^{-8}
Closed Eqs. (23,24)	8.412×10^{-7}	-1.243×10^{-9}	1.627×10^{-8}	9.250×10^{-8}	1.897×10^{-7}

*F_{166}, F_{266} estimated from test data in Table 6 (no constraint conditions).
**F_{166}, F_{266} estimated from test data in Table 8 (no constraint conditions).

Table 6

Summary of Test Data Used to Evaluate Interaction Parameters for 3M SP288-T300

Laminate	Test Condition	σ_1 MPa	σ_2 MPa	σ_6 MPa
90°	Compression-torsion*	0	-81.278	80.637
90°	Compression-torsion*	0	-43.280	83.912
0°	Tension-torsion*	66.623	0	101.246
0°	Tension-torsion*	61.611	0	98.061
90°	Internal pressure -axial compression*	160.8	-120.663	0
0°	Tension-tension*	187.2	48.265	0
0°	Biaxial-cross (Ref. 2)	-184.7	-77.914	0

*Tubes, R = 2.525 cm

Table 7

Combined Loading Failure Tests for IM7/8551-7

Laminate†	Test Condition	σ_1 (MPa)	σ_2 (MPa)	σ_6 (MPa)
90°	Pressure	137.90	68.74	0
90°	Pressure	131.70	66.19	0
90°	Pressure-compression	224.78	76.54	0
90°	Pressure-compression	590.21	-155.83	0
90°	Pressure-compression	817.75	-124.80	0
90°	Pressure-compression	495.06	64.81	0
0°	Pressure-compression	-448.18	47.58	0
0°	Pressure-compression	-169.62	62.75	0
90°	Torsion-tension	0	11.03	170.31
0°	Torsion-compression	285.45	0	182.03
90°*	Torsion-compression	0	13.79	148.93
90°*	Torsion-compression	0	-33.10	185.48
0°*	Torsion-tension	20.69	0	177.20

*These results were used for comparison purposes and not for calculating interaction strength parameters.
†See Table 8 for geometry of tubular test specimens.

Table 8

Geometry of IM7/8551-7 Test Specimens

Test	Specimen	Length (cm)	Width (cm)	Radius (cm)	Thickness (cm)	
0° Tension	C	15.24	1.27	-	0.0559	(4 ply)
0° Compression	C	1.59	1.27	-	0.1745	(12 ply)
90° Tension	C	15.24	2.54	-	0.2301	(16 ply)
90° Compression	C	1.59	2.54	-	0.2253	(16 ply)
90° Torsion*	T	10.16	-	2.55	0.0523	(4 ply)
0° Torsion**	T	10.16	-	2.56	0.0785	(6 ply)

C = coupon, T = tube
*Same nominal geometry for combined tests (e.g., torsion-tension, compression-pressure)
**Same nominal geometry for combined tests

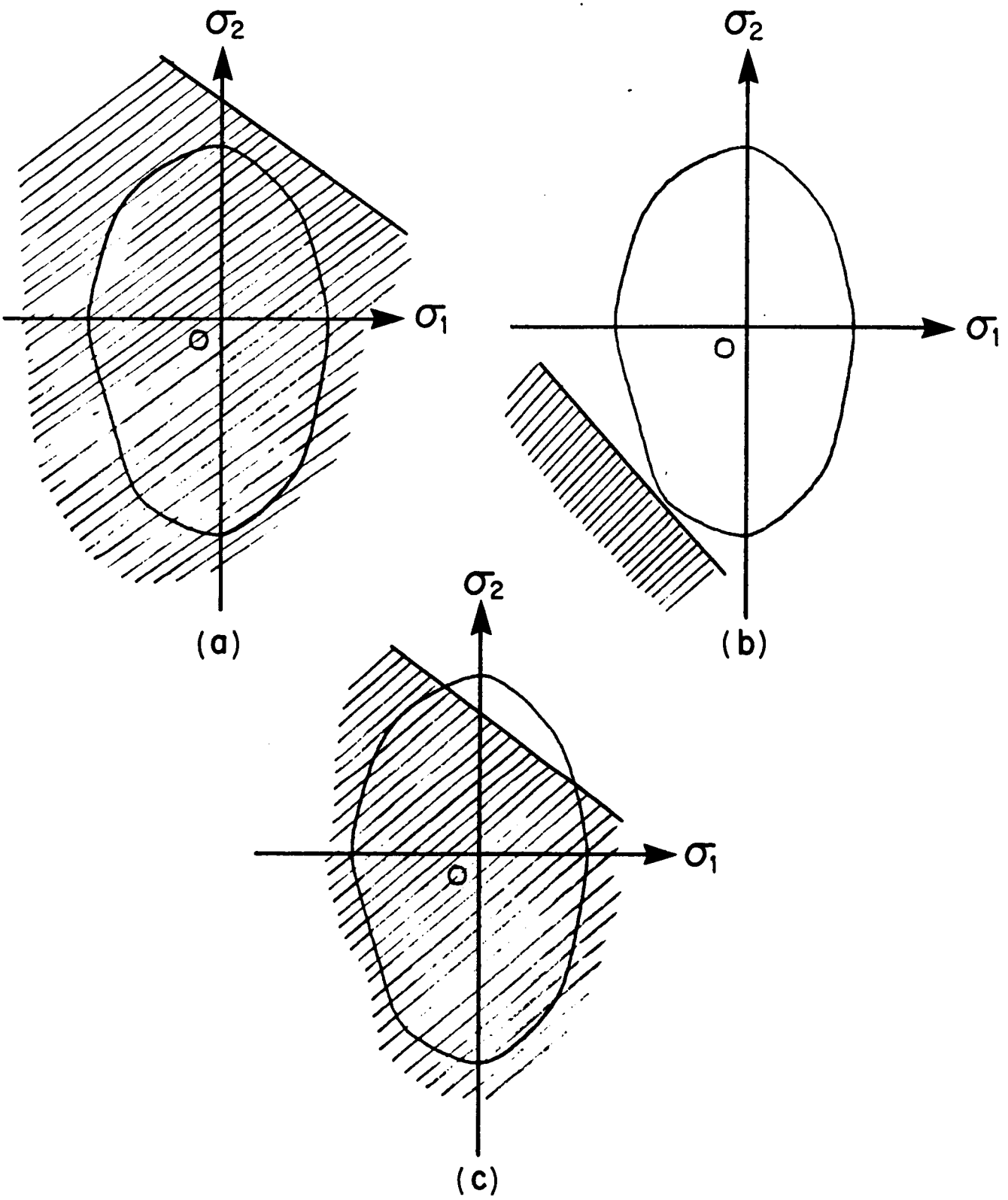

Fig. 1

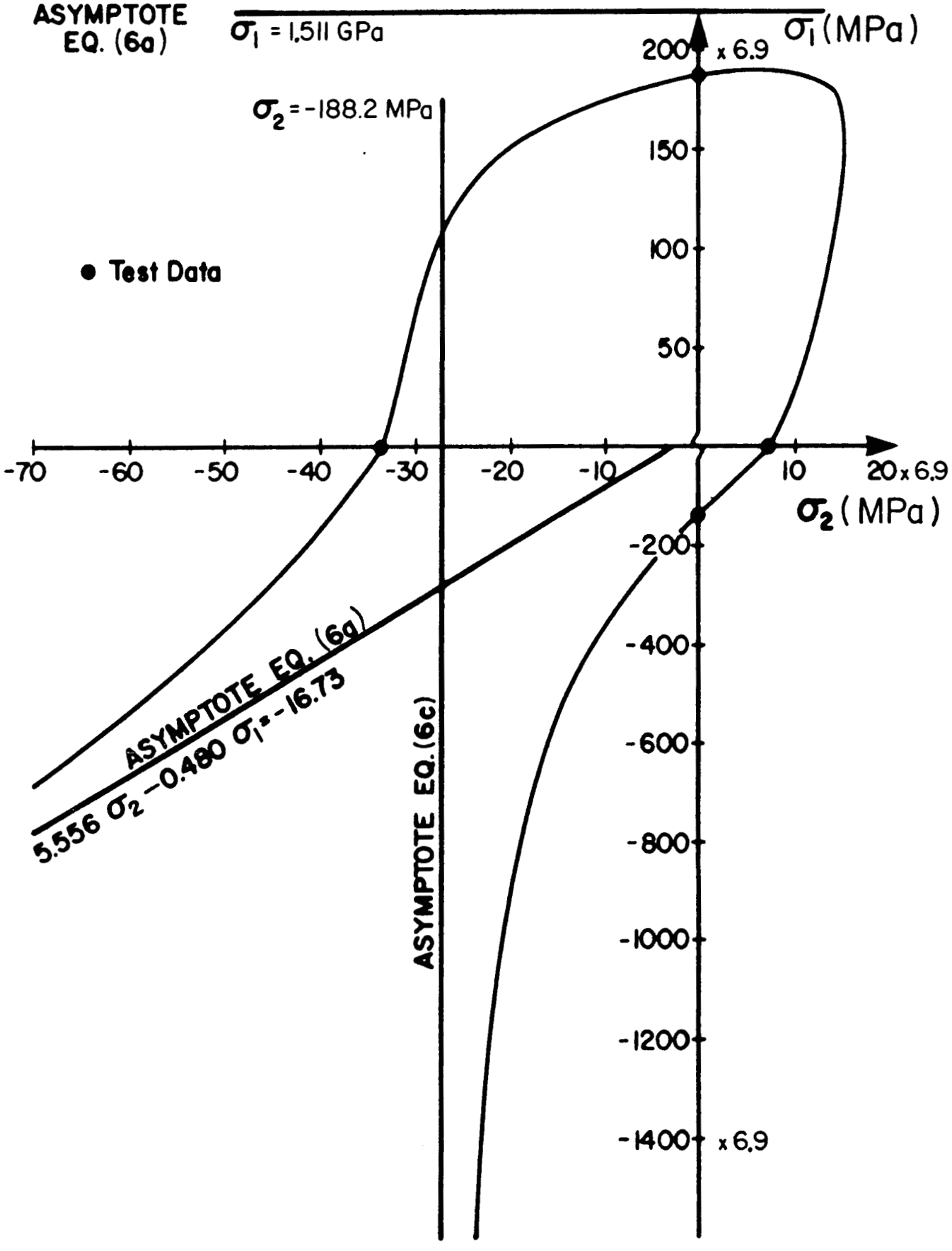

Fig. 2 Penetration of $\sigma_1 - \sigma_2$ Failure Curve by Asymptotes

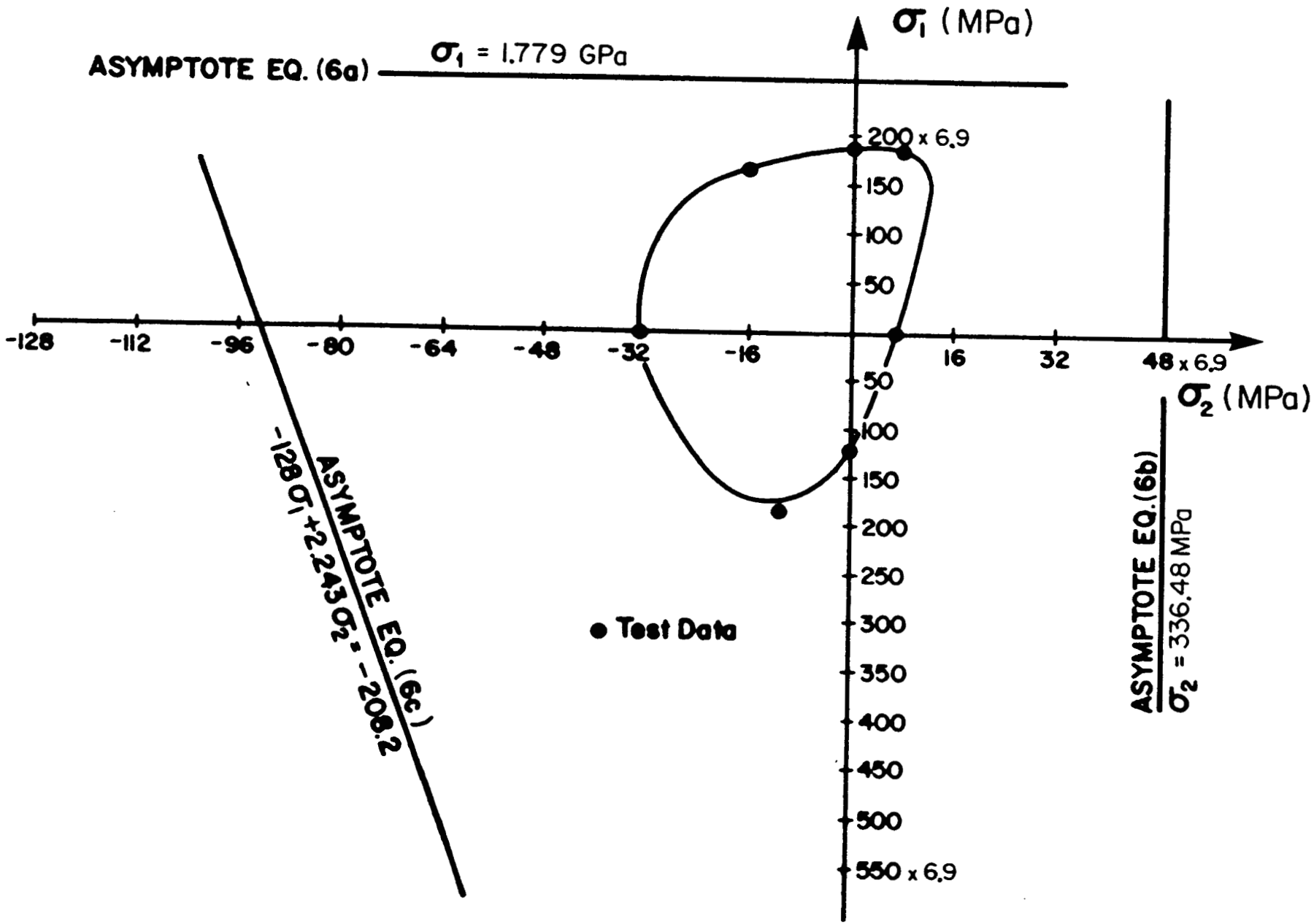

Fig. 3 Closure of $\sigma_1 - \sigma_2$ Failure Curve Using Additional Test Data

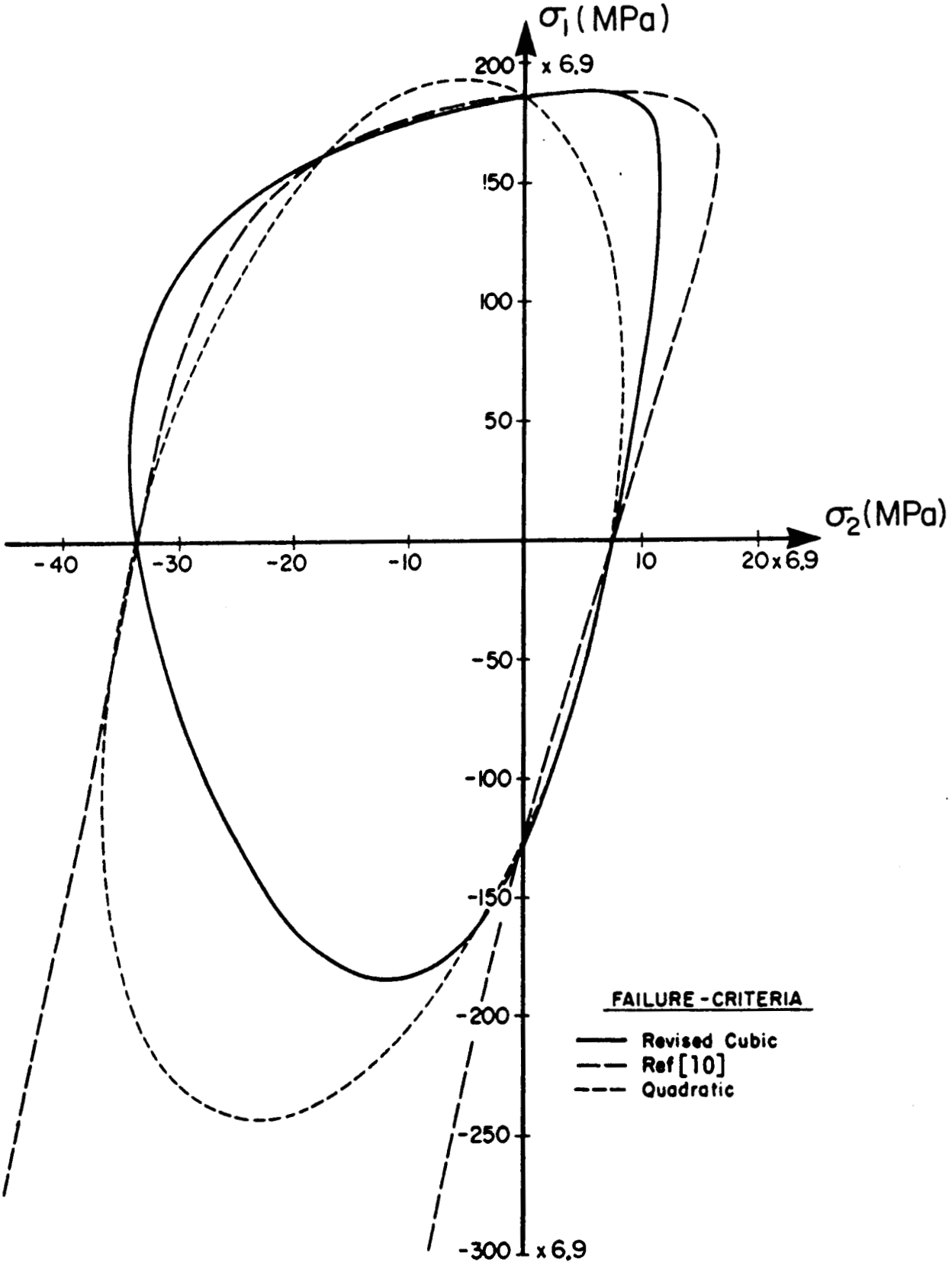

Fig. 4 Planar Failure Surface, $\sigma_6 = 0$

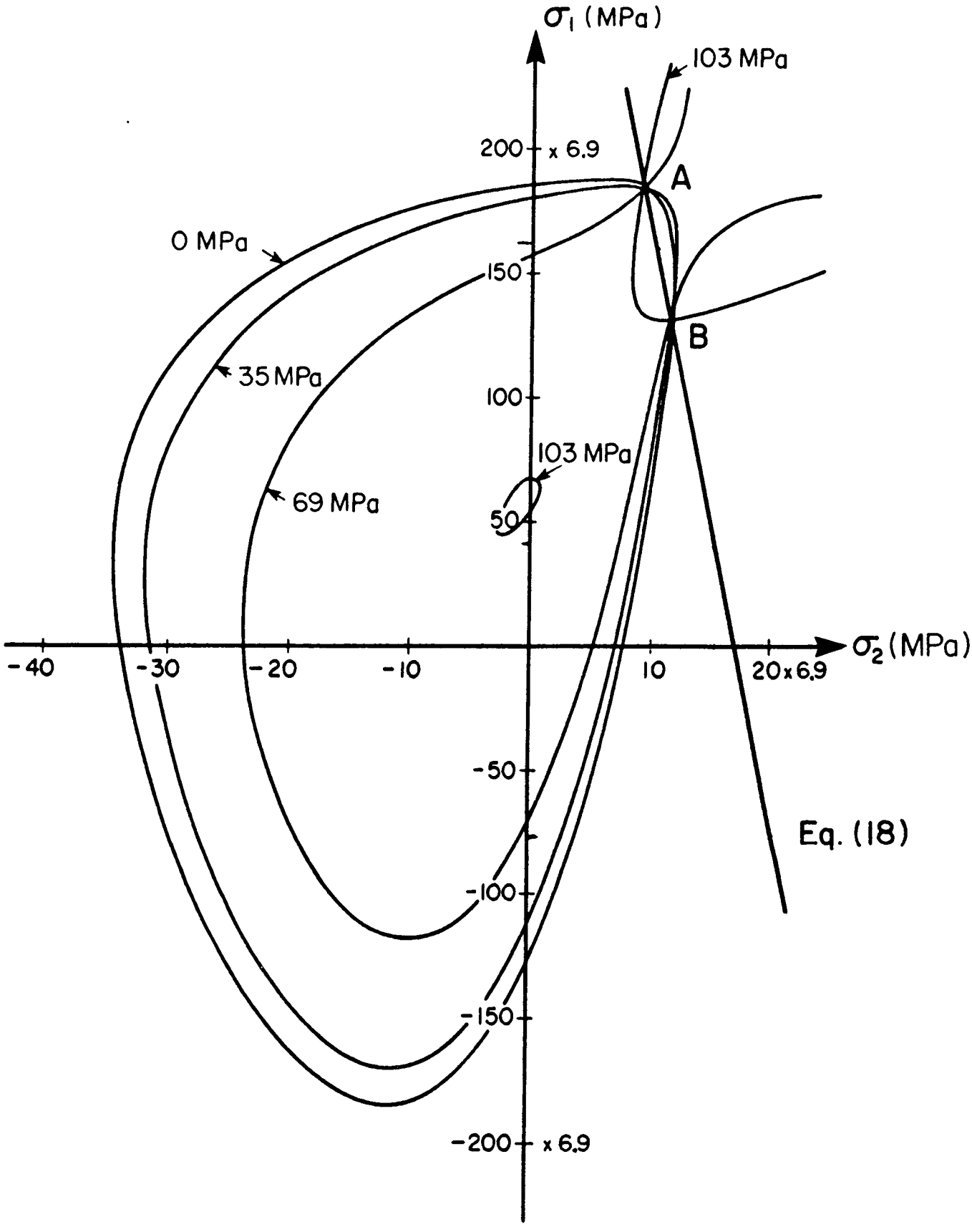

Fig. 5 Failure Surface Contours for Varying σ_6

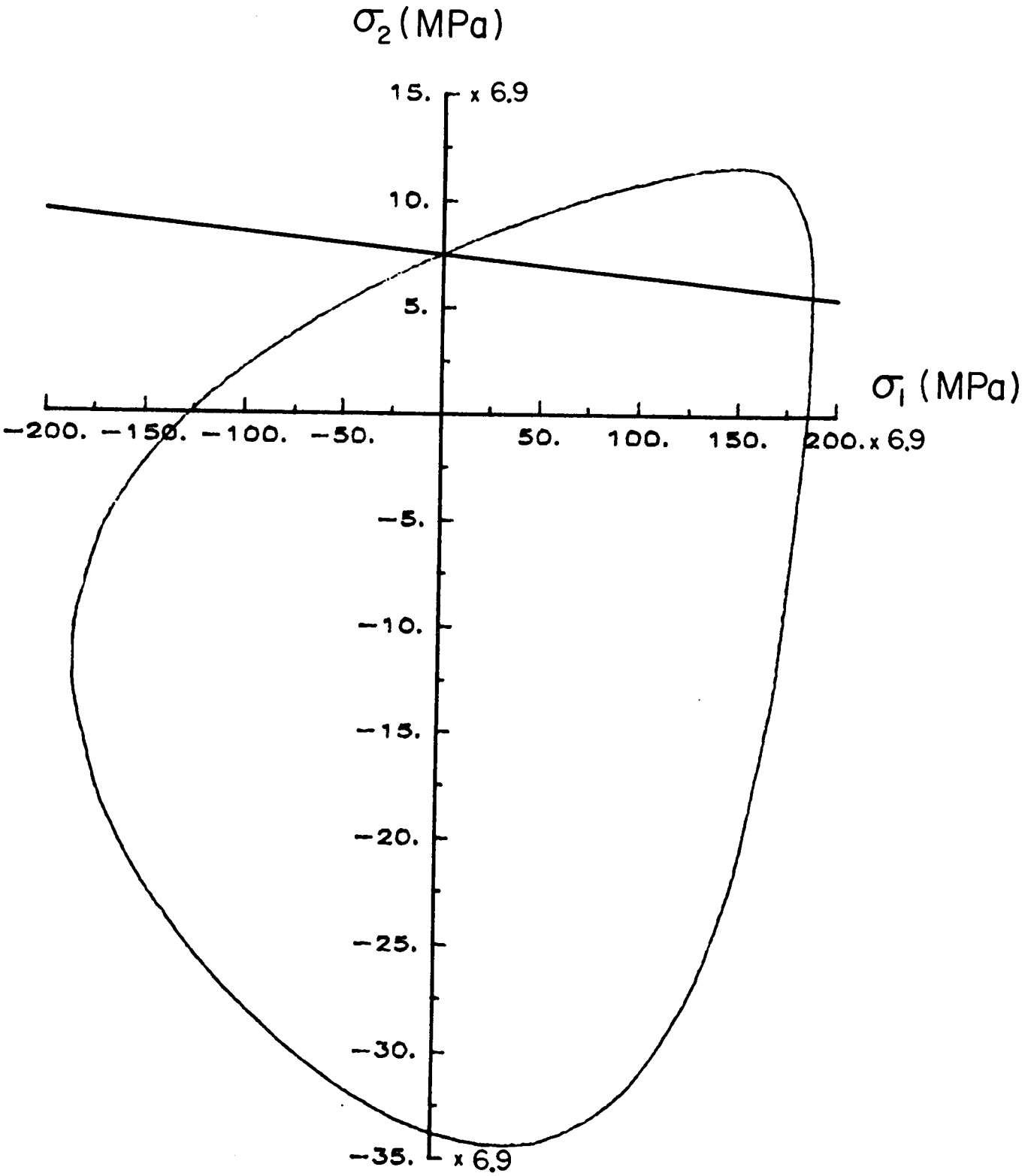
σ2 (MPa)
15.
x 6.9
10.
5.
σ1 (MPa)
-200.
-150.
-100.
-50.
50.
100.
150.
200.
x 6.9
-5.
-10.
-15.
-20.
-25.
-30.
-35.
x 6.9

Fig. 6

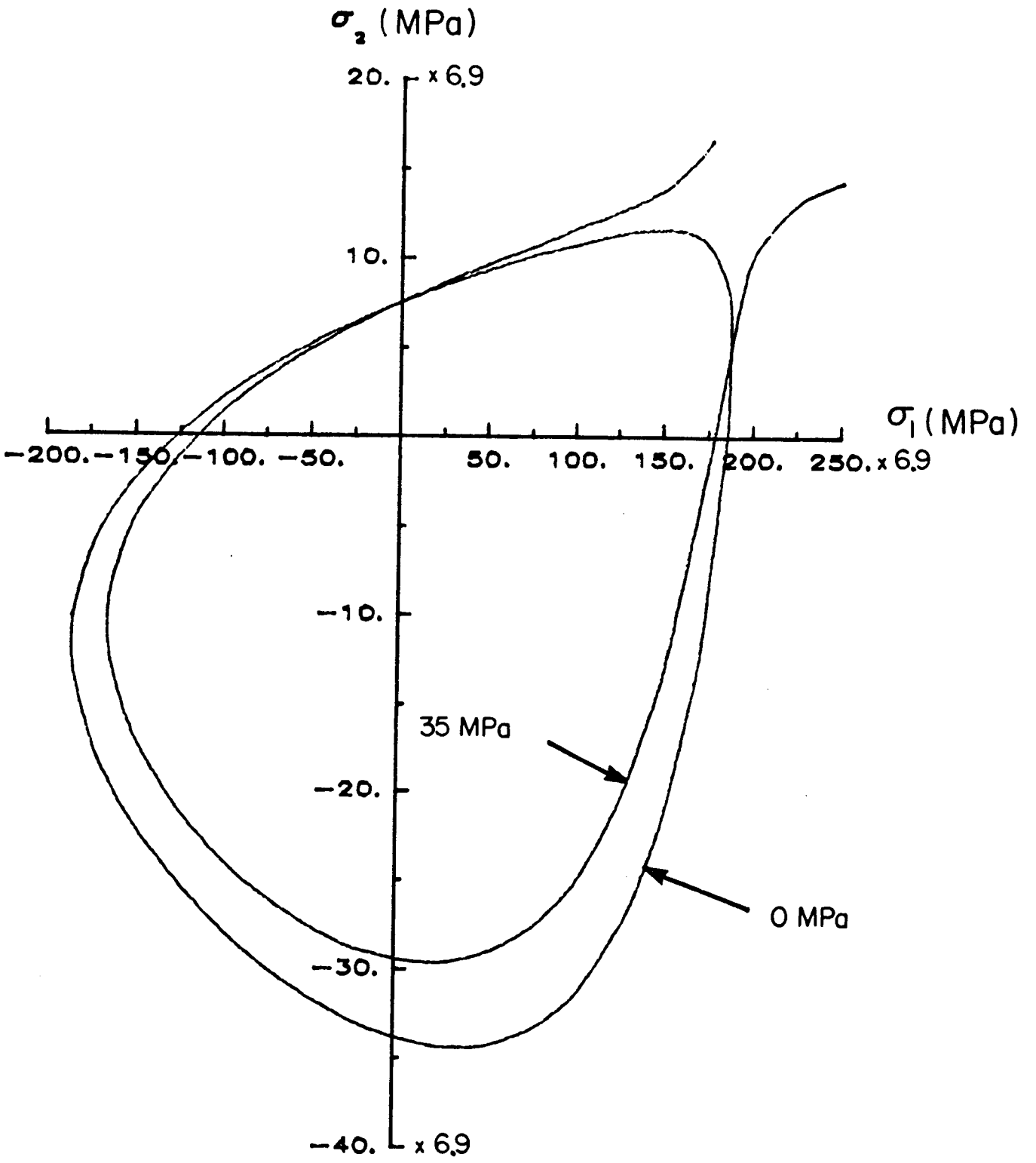
σ2 (MPa)
20.
x 6.9
10.
σ1 (MPa)
−200. −150. −100. −50.
50. 100. 150. 200. 250. x 6.9
−10.
35 MPa
−20.
0 MPa
−30.
−40.
x 6.9

Fig. 7

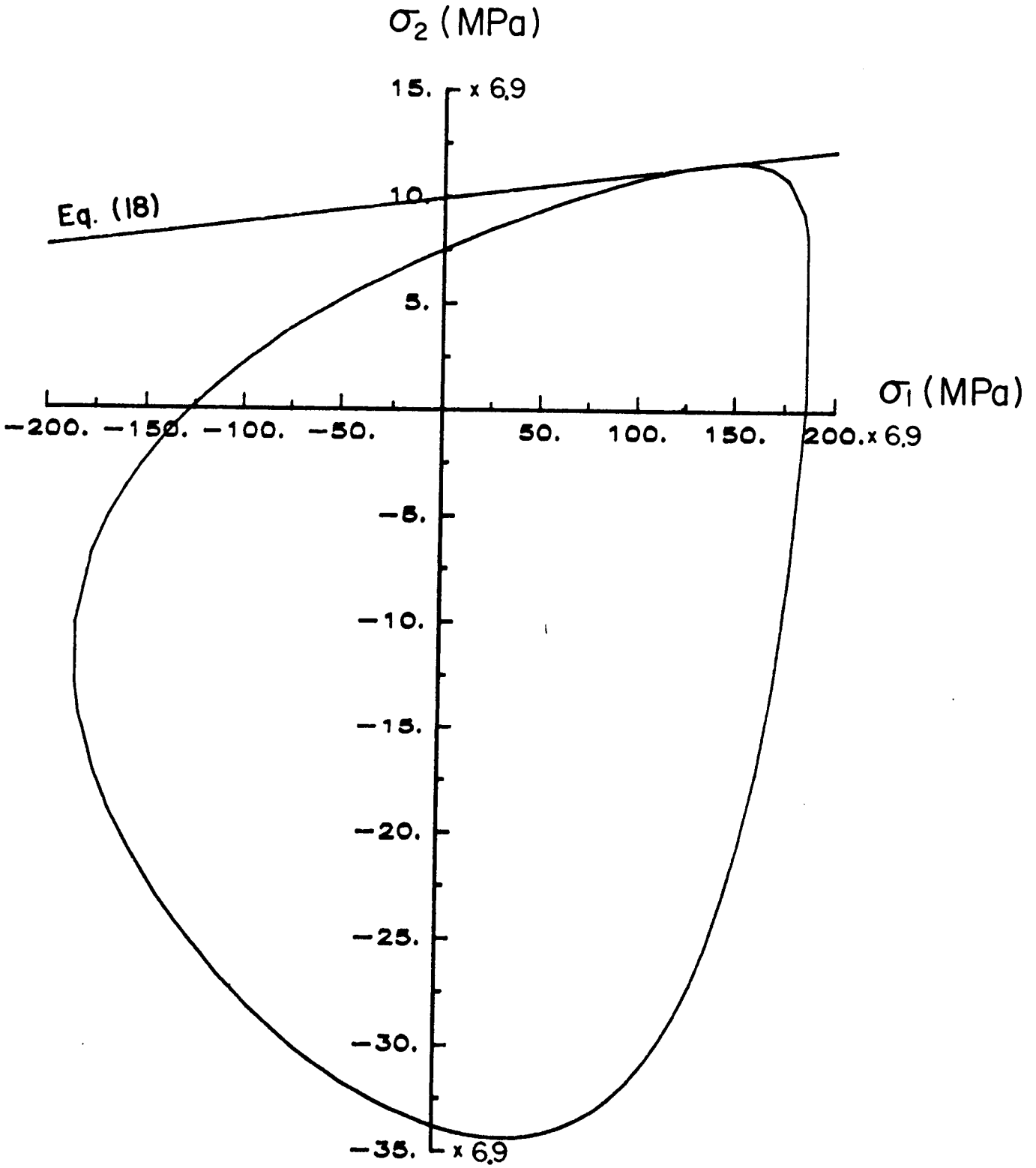
σ2 (MPa)
15.
x 6.9
10.
5.
Eq. (18)
σ1 (MPa)
-200.
-150.
-100.
-50.
50.
100.
150.
200.
x 6.9
-5.
-10.
-15.
-20.
-25.
-30.
-35.
x 6.9

Fig. 8

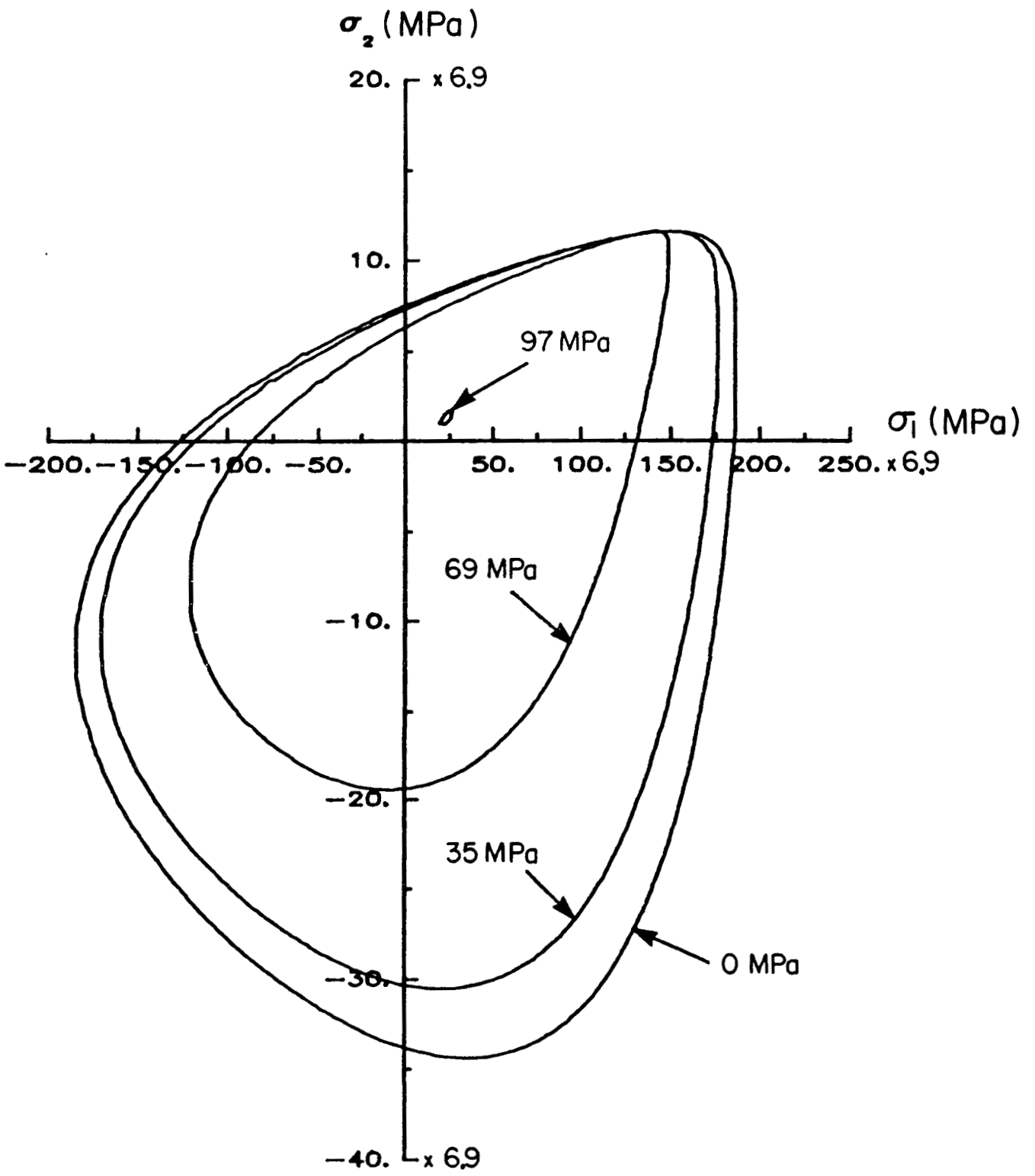

Fig. 9 Closed Failure Surface for Graphite/Epoxy (3M SP288-T300)

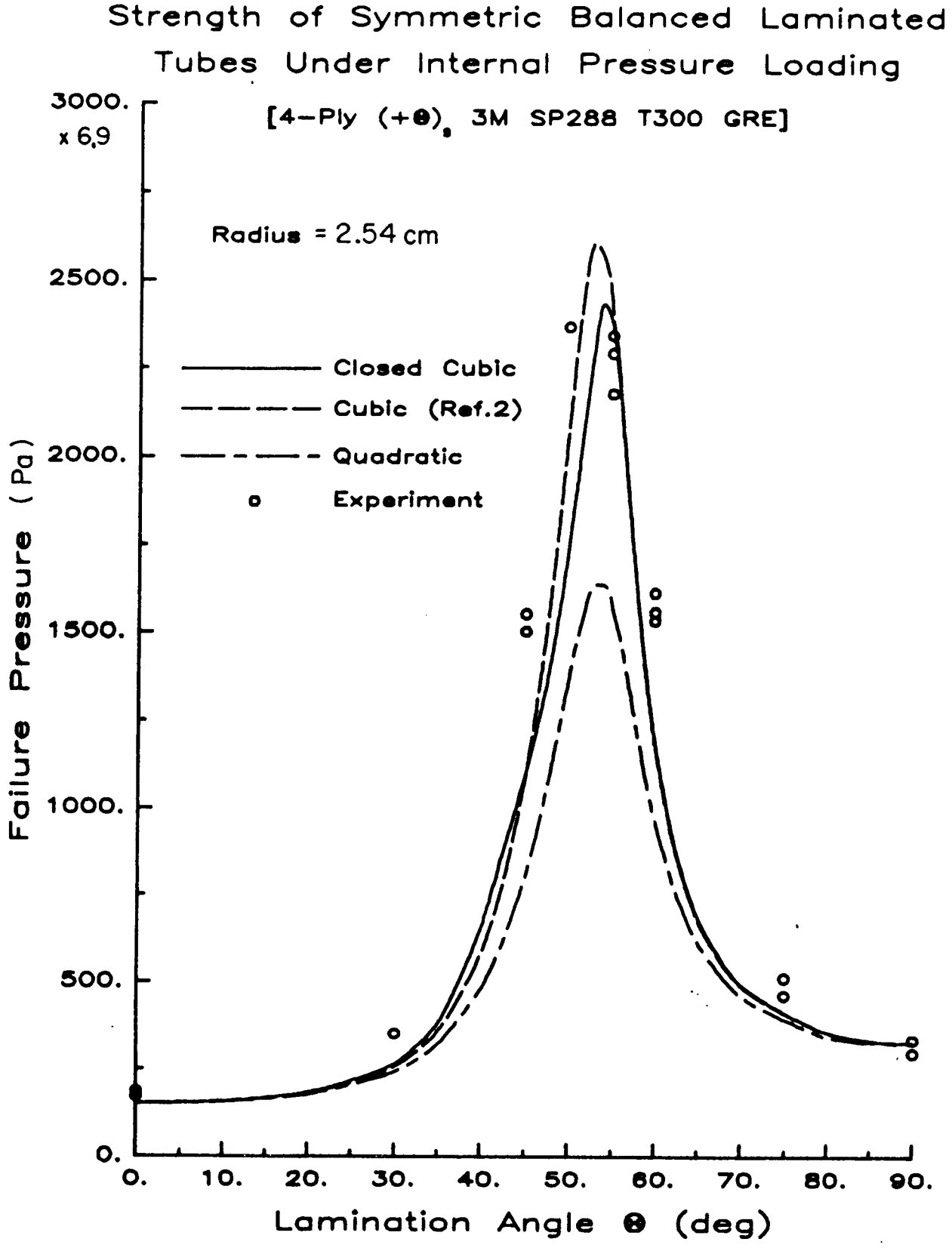
Strength of Symmetric Balanced Laminated Tubes Under Internal Pressure Loading
[4-Ply (+θ)s 3M SP288 T300 GRE]
Radius = 2.54 cm
Closed Cubic
Cubic (Ref.2)
Quadratic
Experiment
Failure Pressure (Pa)
3000.
x 6,9
2500.
2000.
1500.
1000.
500.
0.
0. 10. 20. 30. 40. 50. 60. 70. 80. 90.
Lamination Angle θ (deg)

Fig. 10

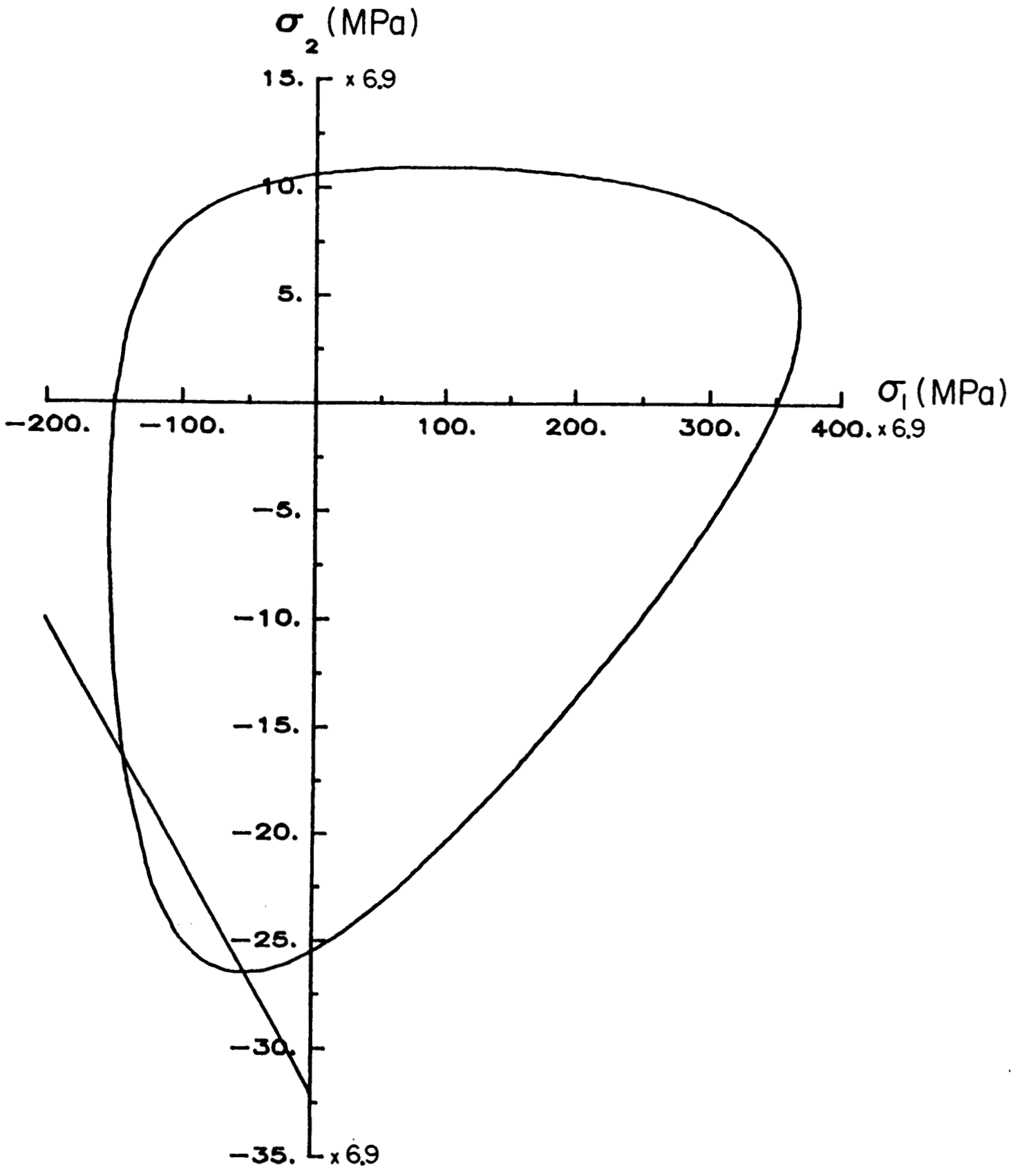
σ2 (MPa)
15.
x 6.9
10.
5.
σ1 (MPa)
-200.
-100.
100.
200.
300.
400.
x 6.9
-5.
-10.
-15.
-20.
-25.
-30.
-35.
x 6.9

Fig. II

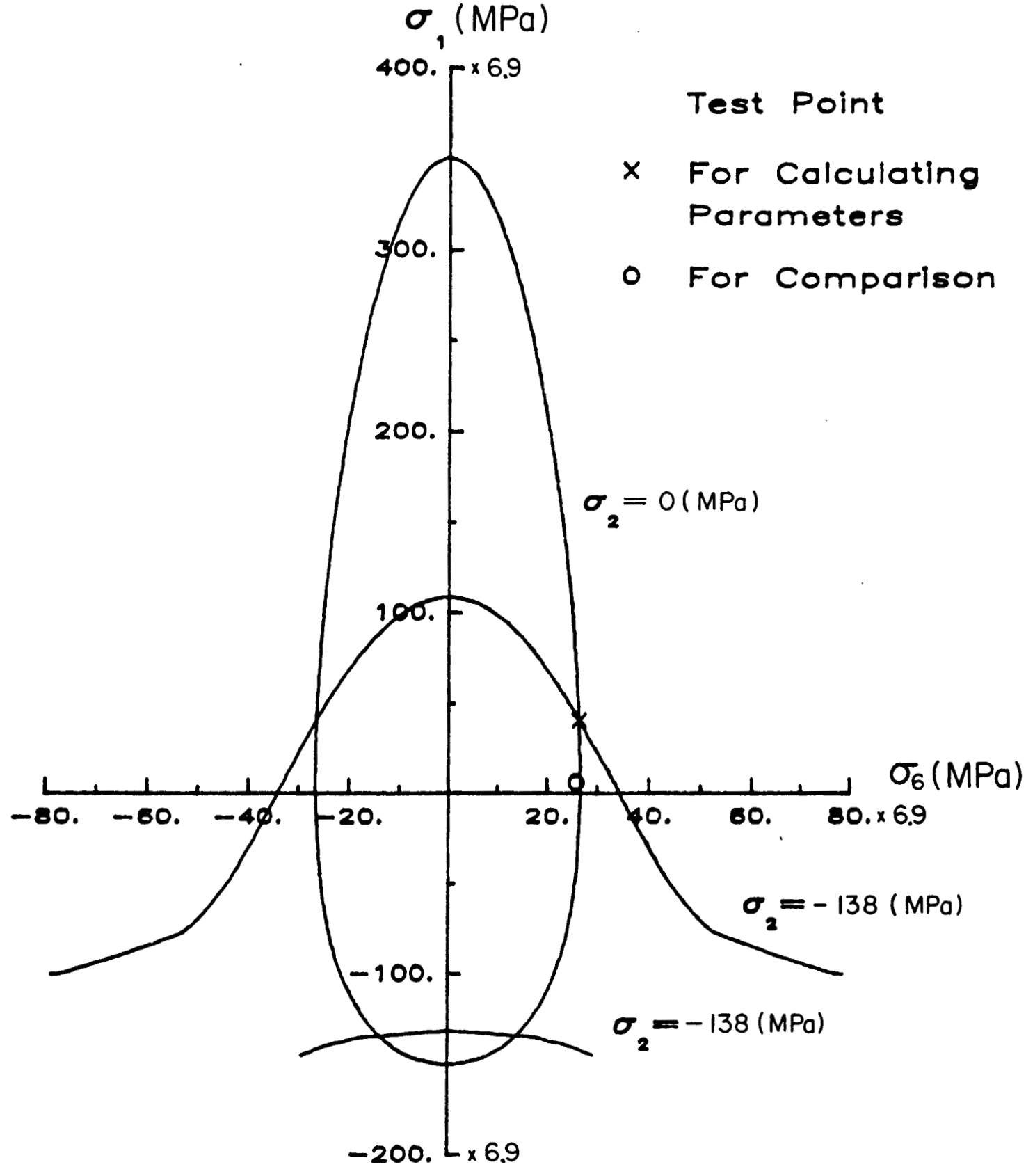
σ1 (MPa)
400.
x 6.9
300.
200.
100.
−100.
−200.
x 6.9
Test Point
x For Calculating Parameters
o For Comparison
σ2 = 0 (MPa)
σ2 = − 138 (MPa)
σ2 = − 138 (MPa)
σ6 (MPa)
−80.
−60.
−40.
−20.
20.
40.
60.
80.
x 6.9

Fig. 12

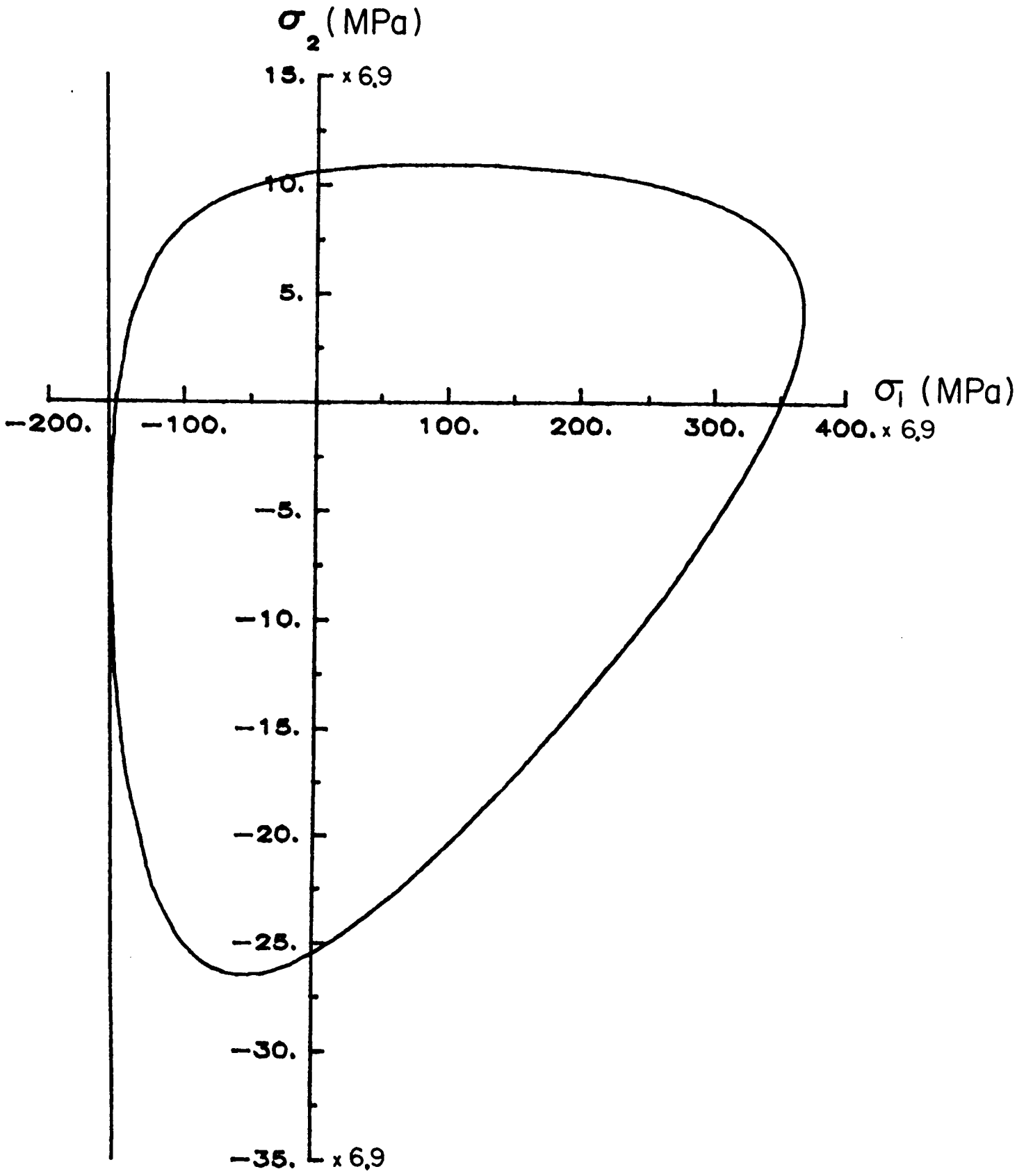
σ2 (MPa)
15.
x 6.9
10.
5.
σ1 (MPa)
-200.
-100.
100.
200.
300.
400.
x 6.9
-5.
-10.
-15.
-20.
-25.
-30.
-35.
x 6.9

Fig. 13

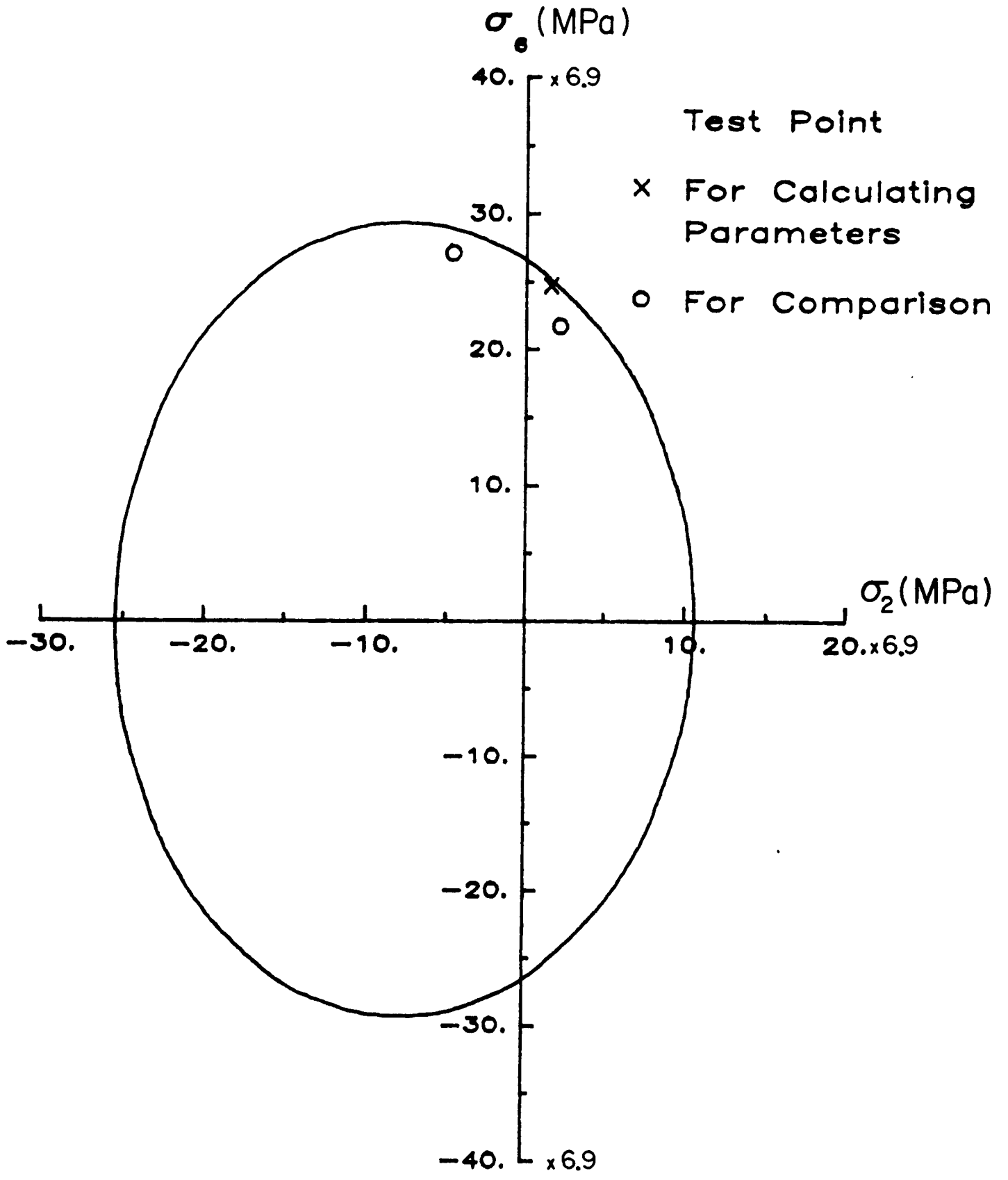
σ_6 (MPa)
40.
x 6.9
30.
20.
10.
−10.
−20.
−30.
−40.
x 6.9
−30.
−20.
−10.
10.
20.x6.9
σ_2 (MPa)
Test Point
× For Calculating Parameters
o For Comparison

Fig. 14

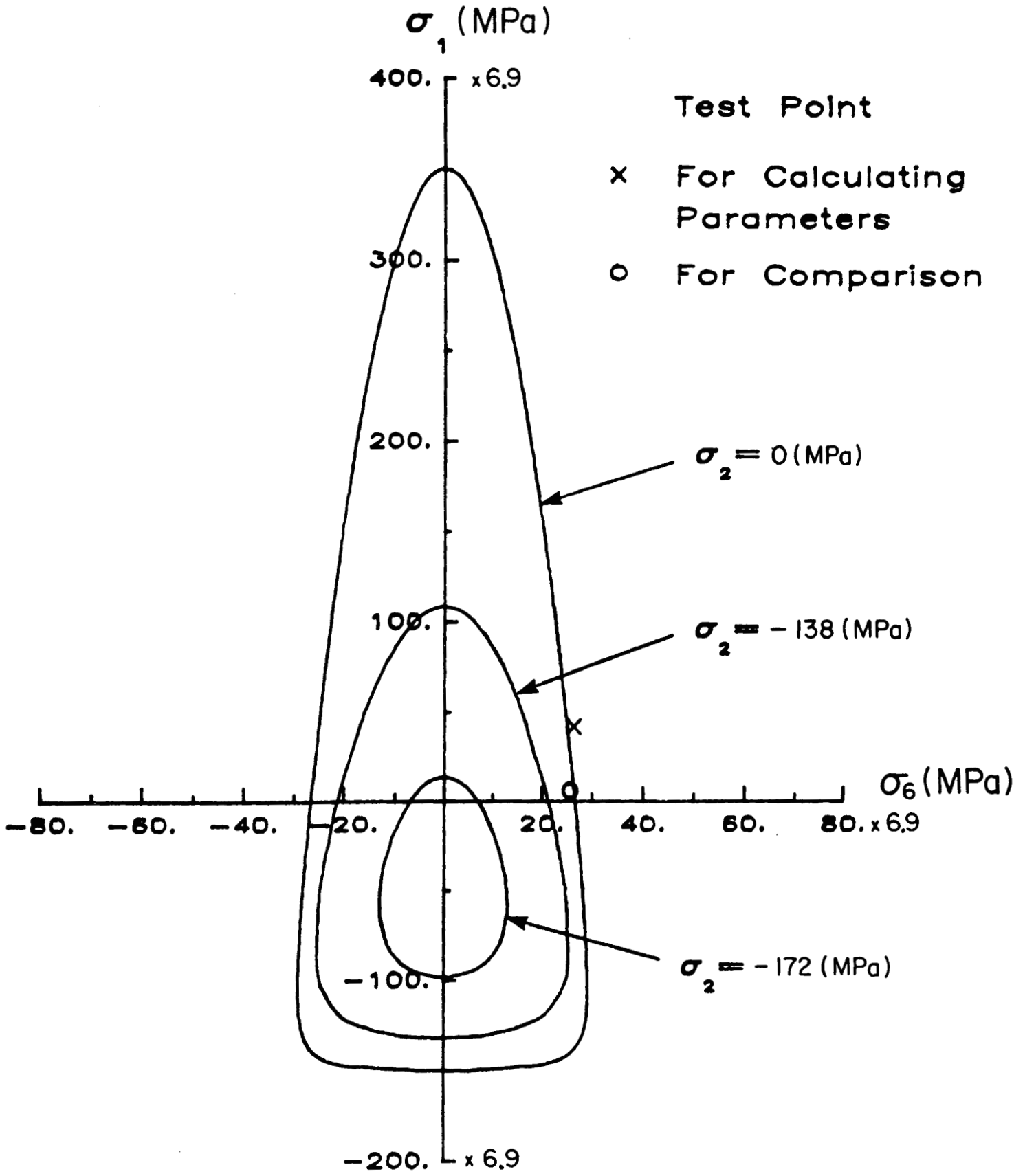

Fig. 15 Closed Failure Surface for Graphite / Epoxy (Hercules IM7/8551-7)